Pictorial Essay

J Korean Soc Radiol 2023;84(6):1266-1289
https://doi.org/10.3348/jksr.2023.0015
eISSN 2951-0805

JOURNAL of THE KOREAN SOCIETY of RADIOLOGY

Typical and Atypical Imaging Features of Malignant Lymphoma in the Abdomen and Mimicking Diseases

복부 악성 림프종의 영상 소견 및 비슷한 소견을 보일 수 있는 질병들

Jong Eun Kim, MD, So Hyun Park, MD*, Young Sup Shim, MD, Sungjin Yoon, MD

Department of Radiology, Gil Medical Center, Gachon University College of Medicine, Incheon, Korea

ORCID iDs
Jong Eun Kim https://orcid.org/0000-0002-8041-0143
So Hyun Park https://orcid.org/0000-0001-9935-2863
Young Sup Shim https://orcid.org/0000-0002-8214-2904
Sungjin Yoon https://orcid.org/0000-0002-7030-841X

Received February 7, 2023
Revised April 21, 2023
Accepted May 6, 2023

***Corresponding author**
So Hyun Park, MD
Department of Radiology,
Gil Medical Center,
Gachon University
College of Medicine,
21 Namdong-daero 774beon-gil,
Namdong-gu, Incheon 21565,
Korea.

Tel 82-32-460-3060
Fax 82-32-460-3065
E-mail nnoleeter@gilhospital.com

Malignant lymphoma typically presents with homogeneous enhancement of enlarged lymph nodes without internal necrotic or cystic changes on multiphasic CT, which can be suspected without invasive diagnostic methods. However, some subtypes of malignant lymphoma show atypical imaging features, which makes diagnosis challenging for radiologists. Moreover, there are several lymphoma-mimicking diseases in current clinical practice, including leukemia, viral infections in immunocompromised patients, and primary or metastatic cancer. The ability of diagnostic processes to distinguish malignant lymphoma from mimicking diseases is necessary to establish effective management strategies for initial radiological examinations. Therefore, this study aimed to discuss the typical and atypical imaging features of malignant lymphoma as well as mimicking diseases and discuss important diagnostic clues that can help narrow down the differential diagnosis.

Index terms Lymphoma; Abdomen; Multidetector Computed Tomography

INTRODUCTION

Lymphoma is a blood cancer caused by the malignant clonal proliferation of lymphocytes from secondary lymphoid organs, including the lymph nodes, spleen, or mucosa-associated lymphoid tissue (1). The International Classification of Diseases from the World Health Orga-

nization (2022) categorizes malignant lymphoma into Hodgkin's lymphoma (HL) (10%) and non-HL (NHL) (90%) (2). Reed-Sternberg cells are abnormal lymphocytes that are a hallmark of HL (2-4). Lymphoma is clinically classified as high-grade (aggressive) or low-grade (indolent) (2). Although radiological imaging cannot differentiate HL from NHL, CT is an essential imaging modality for evaluation, staging, and follow-up of the involvement of lymph node in lymphoma (3). When lymph nodes are affected, they commonly appear enlarged and show homogeneous enhancement in imaging studies. However, lymphoma can also involve other parts of the body, known as extranodal lymphoma (4). Since extranodal lymphoma can arise in any organ of the body, it can be misdiagnosed as another disease, which delays diagnosis and adversely affects treatment outcomes (4, 5). A review of various lymphoma imaging features can improve radiological interpretation. Therefore, this study aimed to discuss the typical and atypical imaging features of lymphoma and mimicking diseases and discuss important diagnostic clues that can help narrow down the differential diagnosis.

ROLE OF RADIOLOGIC IMAGING

Contrast-enhanced CT and 18-fluorodeoxyglucose (18-FDG) PET/CT are the reference standards for staging and response assessment for lymphoma based on the Lugano classification, which is a modification of the Ann Arbor classification for the anatomic description of disease extent. 18-FDG PET/CT is strongly recommended for staging most lymphomas with high FDG avidity, and CT scan is used for other lymphomas, including small lymphocytic lymphoma/chronic lymphocytic leukemia, marginal zone lymphoma, lymphoplasmacytic lymphoma, and cutaneous T-cell lymphoma (CTCL) (6). MRI is preferred for detecting focal bone lesions, primary central nervous system lymphoma, and leptomeningeal infiltration (4, 6). Additionally, 18-FDG PET/CT-based radiomics is an emerging tool for disease characterization and guiding optimal personalized treatment with a standardized uptake value estimation of tumors (7).

Fig. 1. Multiple enlarged lymph nodes in a 78-year-old female patient with lymphoma presenting with left flank pain.
A, B. Axial (A) and coronal (B) CT images of the portal venous phase show multiple homogeneously enhanced enlarged lymph nodes (arrows) in the mesenteric, aortocaval, and para-aortic regions. In addition, the mesenteric and para-aortic nodal masses encase the mesenteric vessels without luminal narrowing (sandwich sign, arrows). These findings suggest the involvement of lymphoproliferative diseases. The patient was diagnosed with follicular lymphoma based on a laparoscopic mesenteric lymph node biopsy.

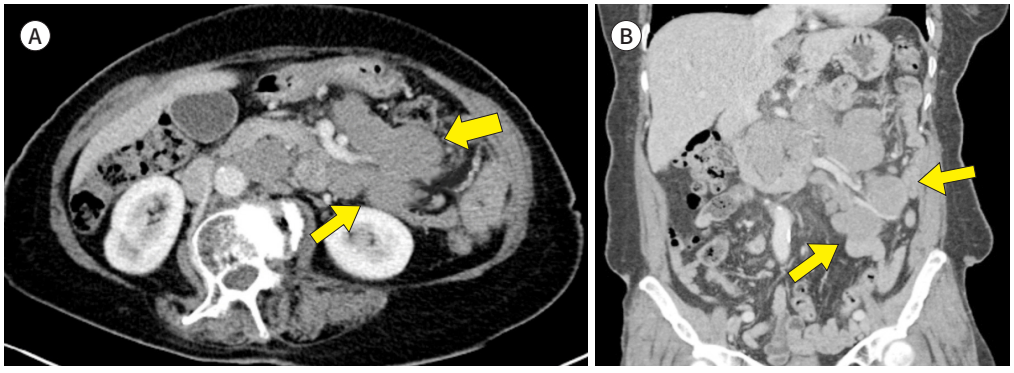

Fig. 2. Lymphoma involving whole-body lymph nodes in a 79-year-old female patient with general weakness and anorexia for 2 months.
A-G. Axial (A) and coronal (B, C) CT images in the portal venous phase show multiple round and ovoid enlarged lymph nodes in the axillary, aortocaval, para-aortic, common hepatic artery, portocaval, common iliac, internal and external iliac areas, and both inguinal areas. Axial (D, E) post-contrast chest CT images show an enlargement of multiple right internal mammary, axillary, mediastinal, and hilar lymph nodes. Additionally, axial (F, G) post-contrast CT of the head and neck show multiple enlarged lymph nodes with cystic or necrotic changes in the submental, submandibular, and neck areas. Percutaneous ultrasound-guided biopsy was performed for a palpable neck mass (not shown) and diffuse large B-cell lymphoma was diagnosed by pathological confirmation.

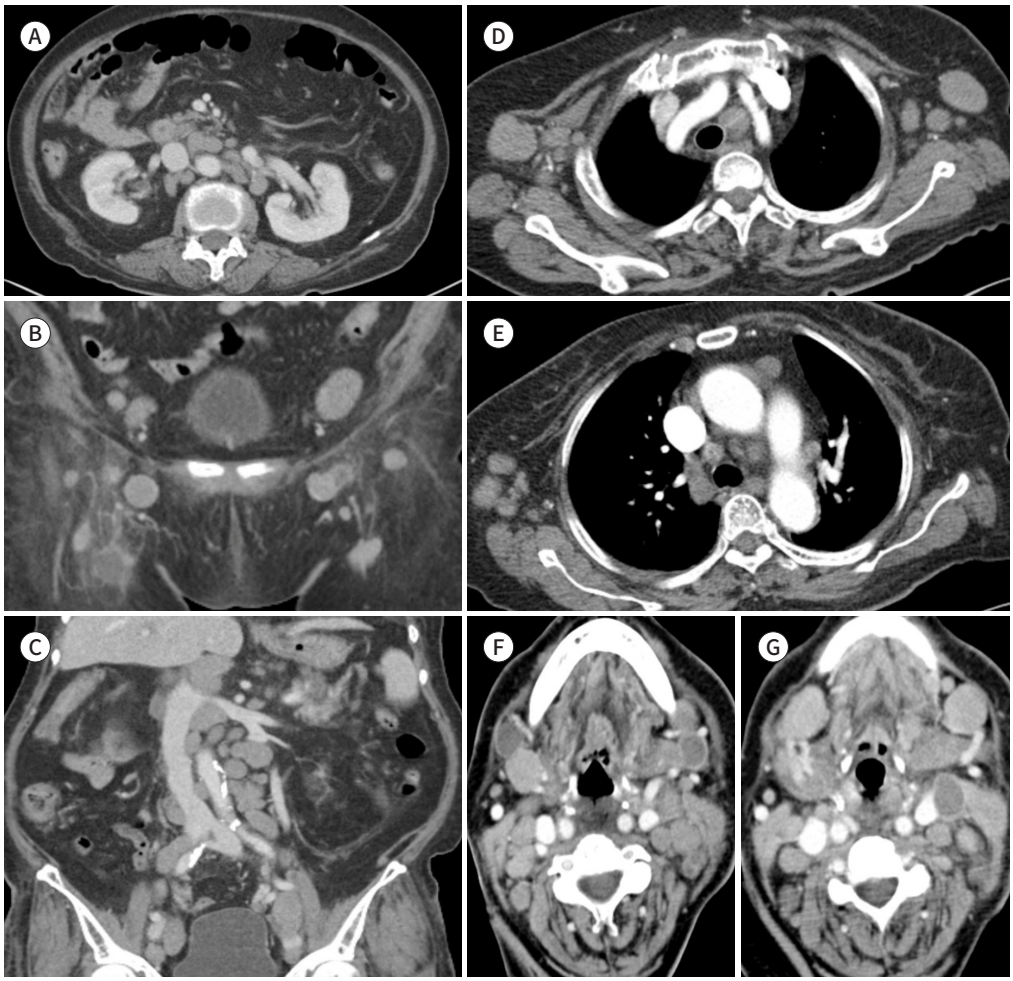

Regardless of the lymphoma site, the typical imaging features are as follows: hypovascularity of the masses and diffuse infiltrative form, lack of vessel steno-occlusion despite the large size of the lesions, and multifocal lesions associated with multiple enlarged lymph nodes.

IMAGING FEATURES OF THE NODAL LYMPHOMA

Nodal lymphoma is the most common form of lymphoma and is a typical form of HL and low-grade NHL (3).

LYMPHOMA WITH TYPICAL HOMOGENEOUS ENLARGED LYMPH NODE

Lymphoma typically presents with homogeneous, mild-to-moderate enhancement of multiple enlarged lymph nodes (Fig. 1) (8, 9). Although the normal upper limit of the size of the

Fig. 3. Necrotic lymph nodes with lymphoma in a 65-year-old female patient with recent abdominal pain.
A-D. Axial (A, B, C) and coronal (D) CT images in the portal venous phase show a 15 cm extent of conglomerated necrotic enlarged lymph nodes with encasement of the superior mesenteric artery and superior mesenteric vein, without occlusion showing "sandwich sign" (arrows) and contact duodenum from the third to fourth portion and proximal jejunum. Malignant lymphoma is rarely associated with necrotic or cystic-changed lymphadenopathy. The patient underwent an endoscopic biopsy of the third portion of the duodenum and was diagnosed with high-grade B-cell lymphoma.

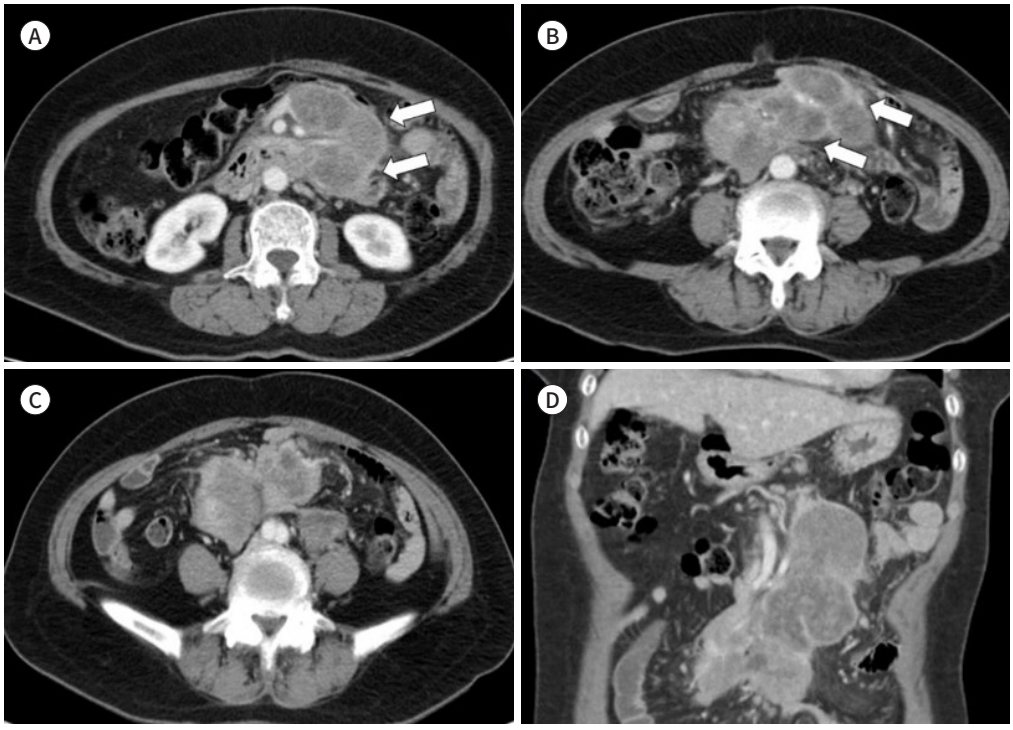

Fig. 4. Necrotic lymph nodes with lymphoma in a 36-year-old female patient with recent abdominal pain.
A-C. Axial (A, B) and coronal (C) CT images in the portal venous phase show multiple enlarged lymph nodes in the retrocrural, aortocaval, and para-aortic areas. Although some lymph nodes contain internal necrotic changes (arrows), the general feature of homogeneous enhancing lymph nodes without a venous occlusive effect, despite a large tumor volume, suggests that lymphoma is more likely than other metastatic lymph nodes or tuberculous lymphadenitis. Surgical left iliac lymph node biopsy was performed, and high-grade B-cell lymphoma was confirmed by pathological examination.

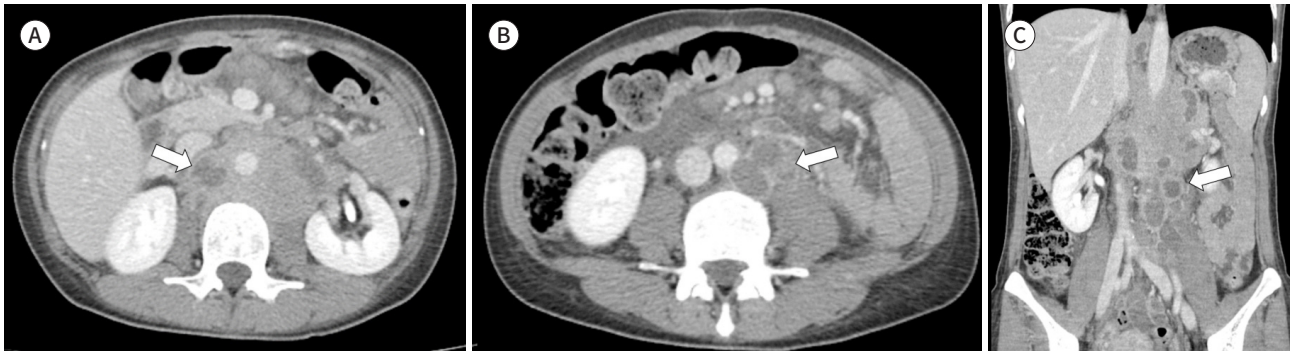

JOURNAL of
THE KOREAN SOCIETY of
RADIOLOGY

lymph node varies by location (10-12), a lymph node measuring > 1.5 cm in the longest nodal diameter is considered pathological (3). Additionally, mesenteric lymph nodes typically encase the mesenteric vessels without luminal narrowing, resembling sandwich filling due to the lack of a desmoplastic reaction. It is a specific sign of mesenteric lymphoma referred to as a "sandwich sign" (13, 14).

LYMPHOMA WITH ATYPICAL HETEROGENEOUS ENLARGED LYMPH NODE

The nodular sclerosis and mixed-cellularity subtypes of HL commonly present with necrosis, which frequently has a desmoplastic reaction (9, 15). Infrequently, large untreated lymph nodes in NHL also demonstrate intranodular cystic or necrotic changes (8), which can develop in patients with lymphoma who have human immunodeficiency virus (HIV) infection. Radiologists can interpret lymphoma involvement when CT images show multiple necrotic enlarged mesenteric lymph nodes with sandwich sign-preserving mesenteric vessels (Figs. 2-4). Extensive necrotic changes in the lymphomatous nodes in HL and NHL can appear, indicat-

Fig. 5. Gastroduodenal B-cell lymphoma in a 65-year-old female with a history of recent abdominal pain.
A, B. Axial (A) and coronal (B) CT images in the portal venous phase show segmental circumferential wall thickening of the stomach antrum and duodenum, causing gastric outlet obstruction, which was initially suggestive of gastric cancer. However, B-cell lymphoma was confirmed by endoscopic biopsy during esophagogastroduodenoscopy. The patient complained of aggravated abdominal pain and jaundice 2 weeks after admission and showed high bilirubin levels (total bilirubin 7.09 mg/dL, direct bilirubin 5.56 mg/dL) in the blood test.
C, D. On follow-up axial (C) and sagittal (D) portal phase CT images, prominent enhancement of the mucosa and focal wall thinning of the gastric antrum is noted, which suggests impending bowel perforation of the gastric lymphoma with tumor bleeding (arrows). An emergency subtotal gastrectomy was performed, and high-grade B-cell lymphoma was confirmed. However, no enlarged lymph nodes were observed on the CT images.

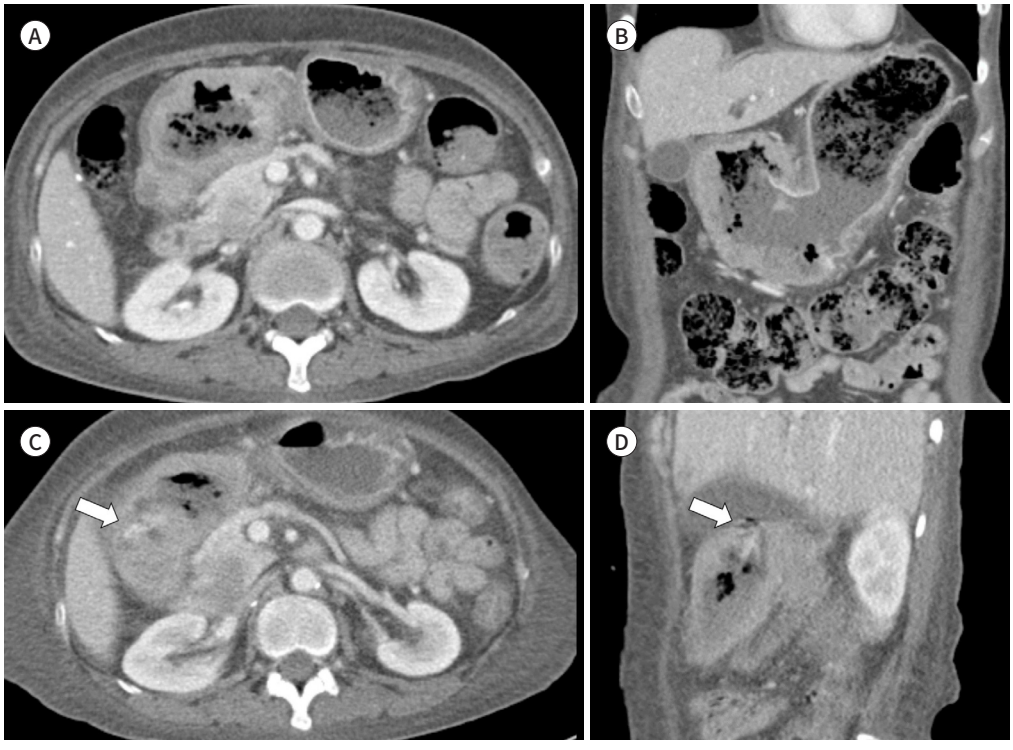

ing a poor survival rate (16-18).

IMAGING FEATURES OF EXTRANODAL LYMPHOMA IN THE ABDOMEN

NHL may present as extranodal lymphoma of any organ (3), whereas extranodal involvement in HL is rare (19).

LYMPHOMA INVOLVING THE GASTROINTESTINAL TRACT

Gastrointestinal (GI) tract lymphoma is the most common type of extranodal NHL lymphoma. However, the imaging features of CT are variable (4).

The most common site of GI NHL (gNHL) is the stomach, followed by the small bowel and colon, and rarely the esophagus (20). Prolonged *Helicobacter pylori* infection is the most common risk factor for gastric involvement in gNHL, which is considered secondary to

Fig. 6. Gastroduodenal B-cell lymphoma in a 56-year-old female with a history of recent epigastric pain and vomiting.
A, B. Axial (A) and coronal (B) CT images in the portal venous phase show segmental circumferential wall thickening of the stomach antrum and duodenum, causing gastric outlet obstruction, which was initially suggestive of gastric cancer.
C, D. On axial (C) and coronal (D) CT images in the portal venous phase, several prominent lymph nodes are observed (< 1 cm) in the left gastric artery and peripyloric areas (arrows), suggestive of metastatic lymph nodes. However, B-cell lymphoma was confirmed by endoscopic biopsy during esophagogastroduodenoscopy.

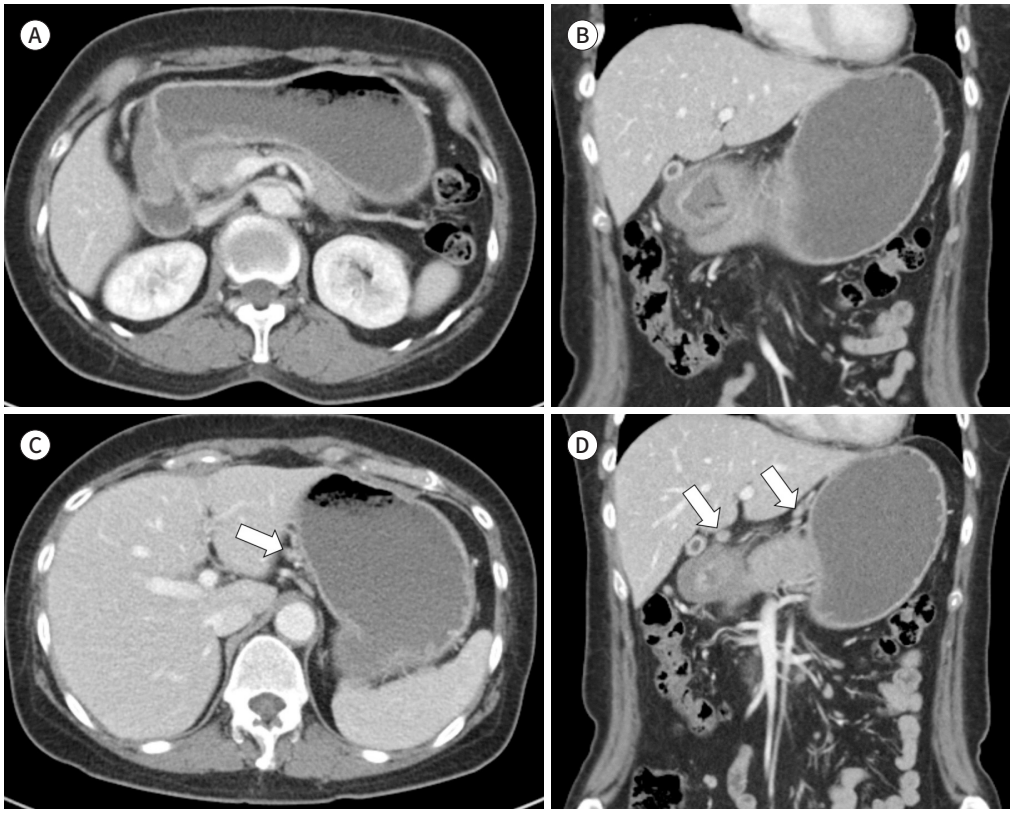

chronic inflammation of the stomach. CT findings include polypoid mass, homogeneous bulky bowel wall or fold thickening, ulcers, pseudoaneurysmal dilatation, and rarely a stenosing mass (21, 22). Aggressive manifestations of gNHL, including GI bleeding, bowel obstruction, and perforation, are uncommon. The absence of intestinal obstruction was due to

Fig. 7. Cecal and appendiceal lymphoma in a 67-year-old male patient with mimicking perforated appendicitis.
A, B. On contrast CT images, homogeneous enhancing wall thickening in the appendix is seen with periappendiceal infiltration and rim (arrows). The patient underwent emergency surgery for suspected perforated appendicitis with abscess formation. However, cecal and appendiceal diffuse large B-cell lymphoma was confirmed after partial cecectomy.

Fig. 8. Subcutaneous T-cell lymphoma in a 25-year-old female patient with suspicion of SLE.
A, B. Axial portal phase CT images reveal multifocal, ill-defined, subtle lesions in the subcutaneous fat layer (arrows). The patient was initially suspected of having SLE because of a facial rash on the left cheek and multiple alopecia on the scalp, and the left cheek lesion was confirmed as panniculitis by punch biopsy. The patient had received SLE treatment for 8 years in the dermatology department, although she did not meet the immunological criteria for SLE. The patient's CT image reveals leukopenia and splenomegaly (not shown). Suspecting a hematologic disorder, the patient underwent bone marrow biopsy and was diagnosed with subcutaneous T-cell lymphoma. After chemotherapy, the facial and subcutaneous fat lesions disappeared.
SLE = systemic lupus erythematosus

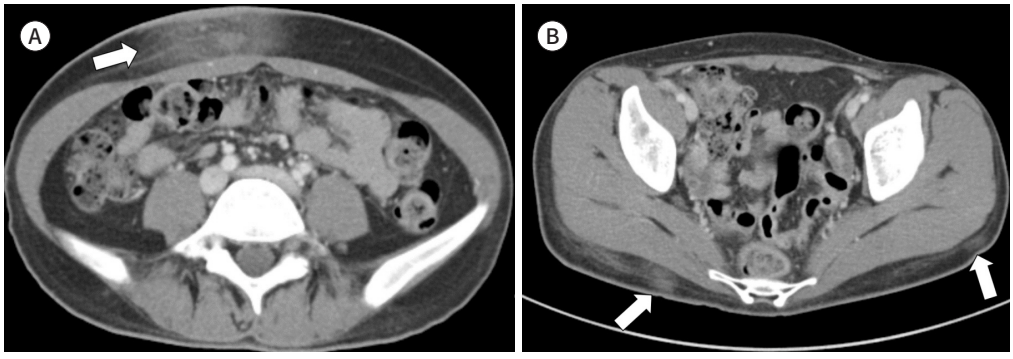

the absence of a desmoplastic reaction in the lymphoma. Additionally, lymphoma invades the muscularis propria and disrupts the autonomic plexus resulting in aneurysmal bowel dilatation (3, 22-24). These findings can aid in the differential diagnosis of lymphoma from adenocarcinoma. However, GI lymphoma rarely presents with gastric outlet obstruction syndrome (Figs. 5, 6), and stenosing masses are a rare manifestation of GI lymphoma (21, 23, 25). Although CT images show bowel stenosis with upstream dilatation, radiologists may suspect lymphoma involvement with multiple enlarged perilesional lymph nodes (> 1.5 cm) without necrosis (3). Gastric cancer is characterized by enlarged necrotic lymph nodes. Additionally, GI stromal tumors do not usually exhibit lymph node metastasis (26).

Primary appendiceal lymphoma is rare and presents as a homogeneously enlarged appen-

Fig. 9. Cutaneous T-cell lymphoma in a 35-year-old female with fever and underlying atopic dermatitis.
A-D. Axial (A) and coronal (B) CT images in the portal venous phase show multiple homogeneously enlarged lymph nodes in both the inguinal and iliac areas. Multiple skin nodules are also present on the axial (C) and coronal (D) portal venous phase CT images (arrows). These findings suggested lymphoma involvement, with suspected combined cutaneous lymphoma. A skin punch biopsy was performed and the skin lesions were cofirmed to be mycosis fungoides, indicating skin involvement in T-cell lymphoma. Percutaneous ultrasound-guided biopsy of the lymph nodes was also performed, and the patient was diagnosed with malignant T-cell lymphoma based on pathological confirmation. The patient was initially diagnosed with atopic dermatitis with systemic erythematous papules and lichen planus at a local clinic 3 years ago and was transferred to the department of dermatology at a tertiary hospital for the management of refractory atopic dermatitis. Skin punch biopsy was performed at that time. The initial pathology results showed acanthosis and superficial dermal perivascular lymphocytic and histiocytic infiltration, suggesting atopic eczema. After reviewing the initial pathology, it was found to be consistent with mycosis fungoides and underlying atopic dermatitis.

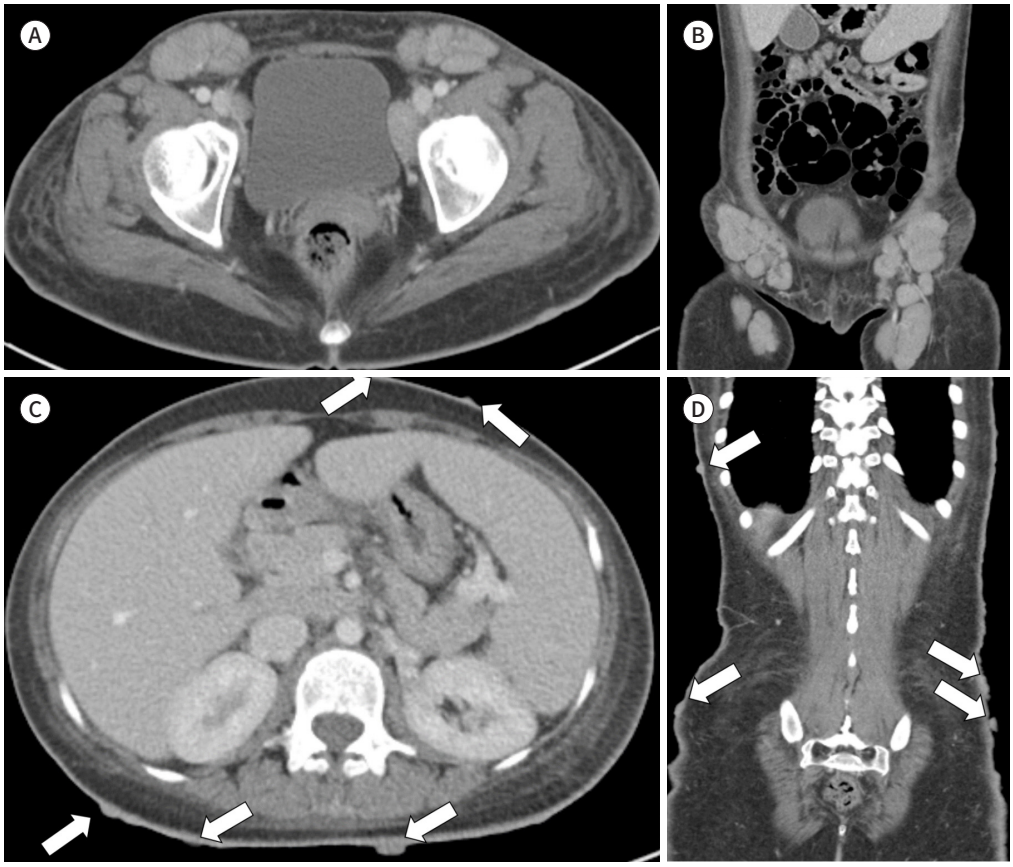

JOURNAL of
THE KOREAN SOCIETY of
RADIOLOGY

dix in CT images of adjacent enlarged lymph nodes. Cecal lymphomas extending to the appendiceal base were more commonly observed on CT images (Fig. 7). Patients with lymphoma involving the appendix experience acute abdominal pain resembling the clinical manifestation of acute appendicitis (12, 22).

LYMPHOMA INVOLVING THE SKIN

Primary cutaneous involvement of lymphoma is rare (4) and is characterized by cutaneous B-cell lymphoma, subcutaneous panniculitis-like T-cell lymphoma (SPTCL) (Fig. 8), and CTCL. Mycosis fungoides is the most common type of CTCL (Fig. 9). Clinical presentation varies with the slow progression of the disease from the patch and infiltrative plaque to the tumor stage, including splenomegaly and lymph node involvement. Although skin lymphoma is difficult to diagnose early because of nonspecific skin thickening or a focal cutaneous nodule or mass, radiologists suspect SPTCL presenting with multiple ill-defined infiltrative lesions in the subcutaneous fat layer with splenomegaly, and CTCL with multiple cutaneous nodules with splenomegaly. The lymph nodes and other extranodal organs are involved in the later

Fig. 10. Retroperitoneal lymphoma with renal and liver involvement in a 90-year-old male with general weakness.
A-D. Axial pre- (A), arterial- (B), portal- (C), and coronal portal- (D) phase images of multiphasic CT present a 14 cm sized, homogeneously enhancing mass with lobulating contour in the right anterior pararenal and perirenal space with infiltration of the right kidney, inferior vena cava (white arrow), and right hemiliver (black arrow). The emergency department initially suspected right renal cell carcinoma because the epicenter of the lesion was the right kidney. However, the mass showed homogeneous enhancement and infiltration of adjacent organs and vessel structures, highly suggestive of infiltrating lymphomas rather than renal cell carcinoma. The mass was diagnosed as B-cell lymphoma using percutaneous transhepatic ultrasound-guided biopsy.

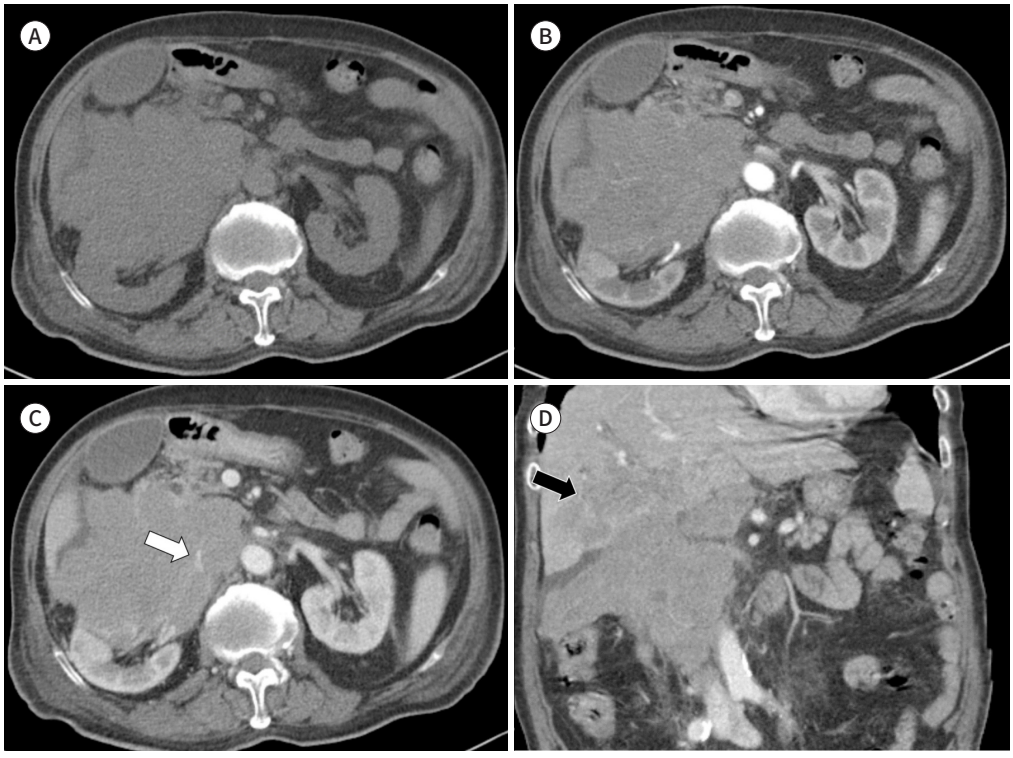

stages of the disease (27). It is easily misdiagnosed as a common skin disease, such as panniculitis from lupus, rather than SPTCL, atopic dermatitis, or psoriasis at the early stage of mycosis fungoides, and the diagnosis is frequently delayed by a median duration of 3 years (28).

LYMPHOMA INVOLVING THE KIDNEY

The prevalent features of renal lymphoma are patent renal arteries and veins despite tumor growth. Renal lymphomas exhibit several distinct patterns. First, diffuse infiltration of the kidney shows an enlarged kidney with hypodense parenchyma in the early post-contrast phase on CT images (Fig. 10). The atypical growth pattern of renal cell carcinoma (RCC), severe pyelonephritis, and autoimmune or traumatic processes of the kidney mimic the infiltration pattern of renal lymphoma (29). Second, solitary, focal, or multiple intraparenchymal renal hyperdense or hypoattenuating masses can be observed on CT images. The differential diagnosis of nodular involvement includes RCCs, metastatic disease, pyelonephritis, renal abscess, and IgG4-related renal disease. Third, contiguous retroperitoneal lymphoma kidney involvement indicates invasion along the renal capsule or sinus (Figs. 11, 12). Retroperitoneal malignancies, including

Fig. 11. Surgically proven renal lymphoma in a 43-year-old male patient presenting with acute left flank pain.
A-D. Axial (A) and coronal (B-D) portal venous phase CT images show diffuse, ill-defined, and homogeneous masses encasing the left renal artery without occlusion and covering the left renal hilum, left ureter, paraaortic, aortocaval, and both iliac areas, suggesting lymphoma involvement. Left hydronephroureterosis is observed, suggesting obstructive uropathy due to lymphoma that is a cause of acute left flank pain. Elective retroperitoneal mass excision was performed for retroperitoneal mass after CT examination, and the patient was diagnosed with low-grade B-cell lymphoma by pathological confirmation.

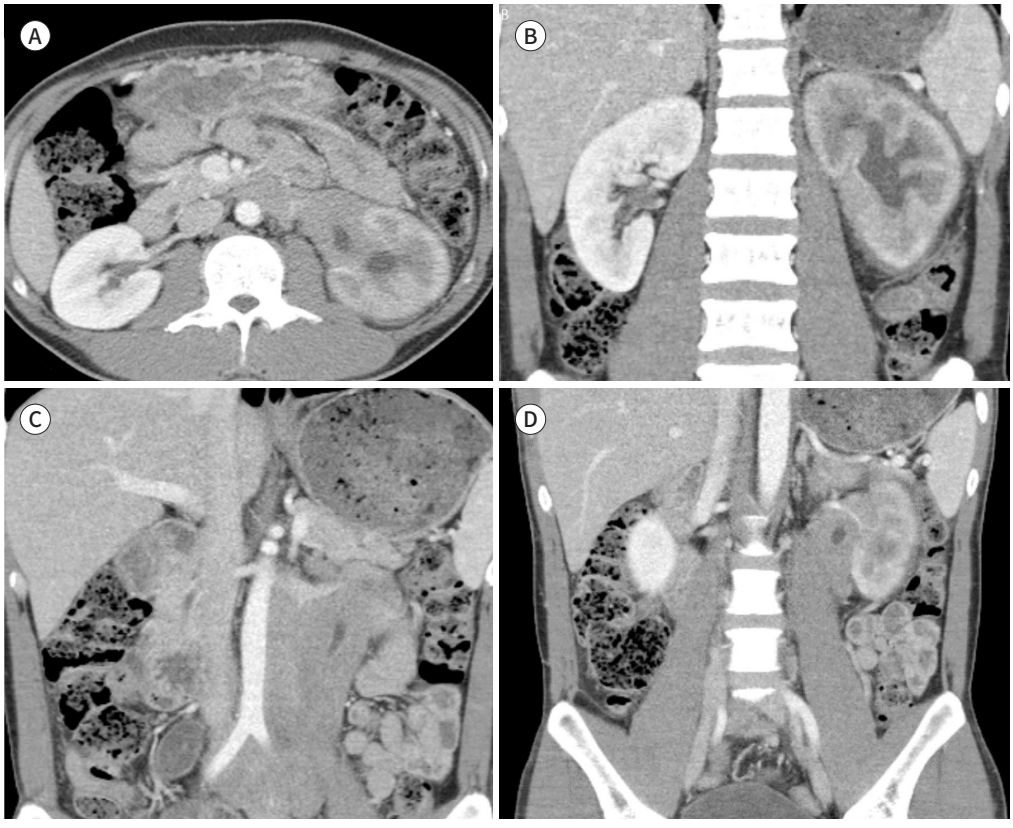

JOURNAL of
THE KOREAN SOCIETY of
RADIOLOGY

sarcoma and metastases, or benign conditions such as perinephric hematoma, retroperitoneal fibrosis, or amyloidosis, can be considered differential (3, 30, 31). The presence of homogeneously enlarged retroperitoneal lymph nodes and splenic disease can help diagnose renal lymphoma (31). The prognosis of lymphoma with renal involvement is poor, and renal dysfunction caused by direct tumor involvement is a poor prognostic factor (32).

LYMPHOMA INVOLVING THE LIVER

Hepatic lymphomas present with primary or secondary liver involvement. Primary hepatic HL is extremely rare and two types are predominantly present in NHL (12, 33). Primary hepatic lymphomas are rare, accounting for < 1% of extranodal lymphomas (3). There are various patterns of hepatic involvement in lymphoma, the most common being diffuse infiltration or multiple hypodense lesions. Other features include large solitary heterogeneous or hypodense masses and miliary patterns (< 1 cm in diameter) in patients with hepatic lymphoma (3, 12, 33). Primary hepatic lymphoma occurs as a solitary mass, whereas multiple nodular primary lymphomas in the liver can occur with a poor prognosis (Fig. 13) (30). Multifocal hepatic lymphomas can mimic metastasis, fungal infections, and granulomatous dis-

Fig. 12. Diffuse soft tissue infiltrating lymphoma in a 75-year-old male with dyspnea caused by large pleural effusion.
A-E. Axial (A-C) and coronal (D, E) CT images in the portal venous phase show diffuse soft tissue infiltration along both kidneys, renal pelvis, ureters, and around mesenteric vessels without obliteration and urinary bladder and peritoneal thickening (white arrows) in the perinephric, periureteric, mesenteric, perivesical, and mesorectal areas, suggesting lymphoma. However, the patient was admitted to the respiratory department because a large right pleural effusion is noted (yellow arrows) and the other lesions were missed in the emergency department. After noticing lymphoma involvement in the formal radiologic report, the patient was transferred to the hematology department. A bone marrow biopsy confirmed non-Hodgkin lymphoma (Waldenstrom's macroglobulinemia).

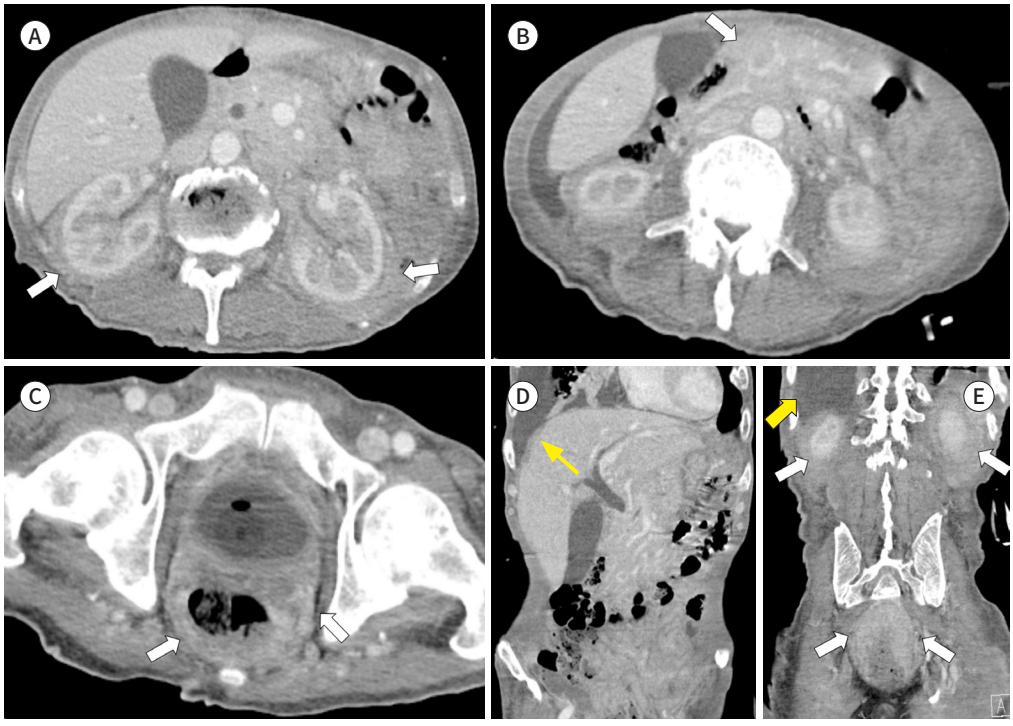

eases (33). Similarly, secondary hepatic lymphoma can present as a solitary hypodense mass, whereas the typical imaging findings of secondary hepatic lymphoma are diffuse (Fig. 14) (30). Differentiating solitary forms of hepatic lymphoma from primary hepatic malignancies and inflammatory pseudotumors can be challenging. The presence of splenomegaly and infra- and/or supradiaphragmatic lymphadenopathy may favor secondary hepatic lymphoma (33).

LYMPHOMA INVOLVEMENT OF THE ADRENAL GLAND

Primary adrenal gland lymphoma is a rare extranodal lymphoma, accounting for 4% of

Fig. 13. Primary hepatic lymphoma in a 53-year-old female patient with elevated liver enzyme on the blood test and a history of ovarian cancer.
A, B. Axial (A) and coronal (B) CT images in the portal venous phase show numerous tiny to small hypoattenuating lesions in both the hemilivers combined with blunting of the liver edge. These findings initially suggested the presence of regenerative or dysplastic nodules in the underlying chronic liver disease or multiple hepatic metastases.
C-G. Gadoxetic acid-enhanced MR images show multiple ill-defined rim-enhancing lesions in both the hemilivers on arterial phase subtraction image (C), without washout on the portal (D) and transitional phases (E), diffusion restriction on the diffusion-weighted (F), and apparent diffusion coefficient map images (G), suggestive of liver malignancy. Percutaneous ultrasound-guided needle biopsy was performed and peripheral T-cell lymphoma was confirmed.

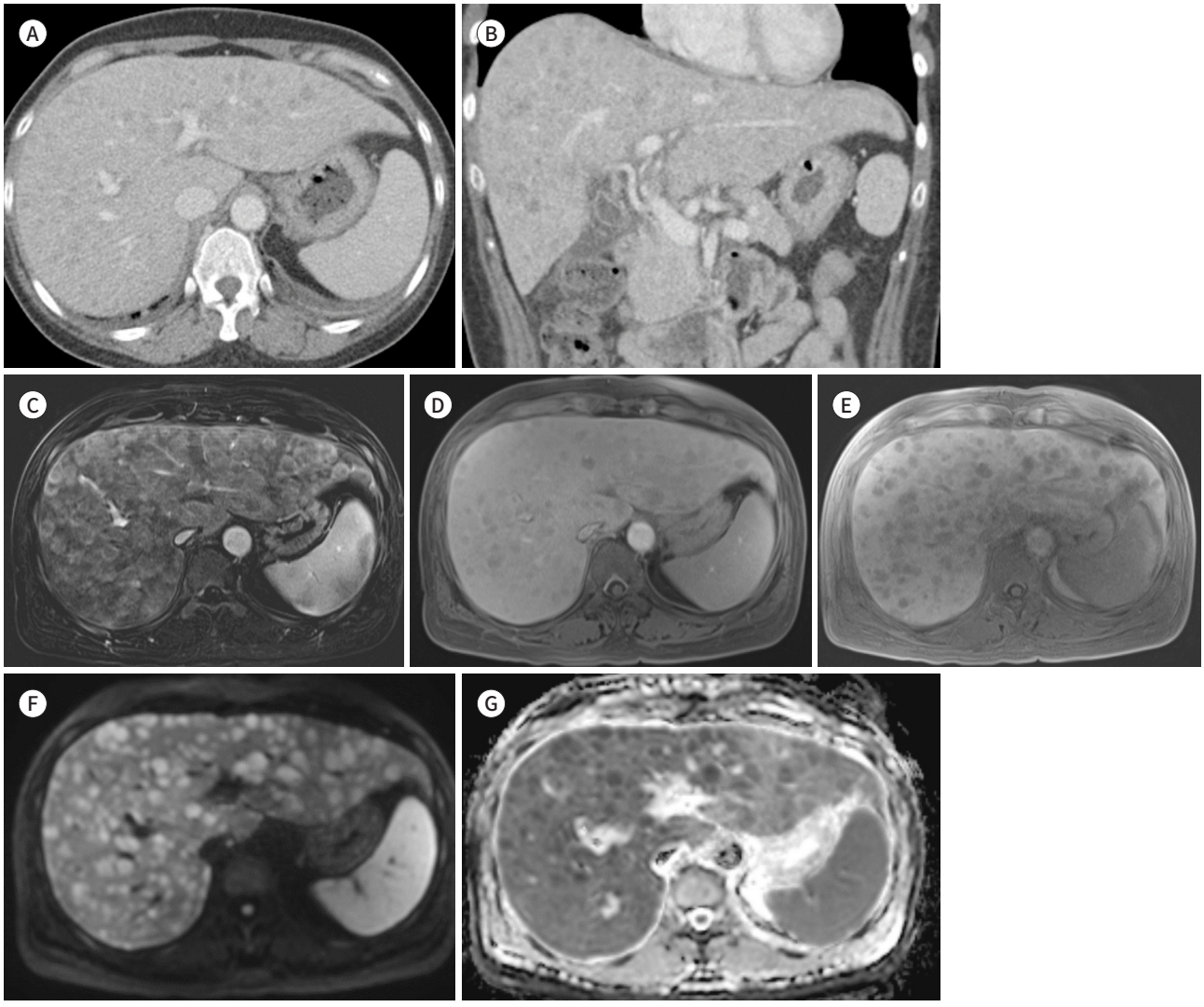

JOURNAL of
THE KOREAN SOCIETY of
RADIOLOGY

Fig. 14. Discrete hepatic nodular lymphoma in a 36-year-old male patient with epigastric pain.
A-D. On axial (A, B) and coronal (C, D) portal phase CT images, a 4.4 cm ill-defined homogeneous subtle low-density lesion (white arrows) is seen in the left lateral segment of the liver. The mass has invaded the left portal vein (black arrow). Multiple enlarged lymph nodes were observed in the left gastric, portocaval, para-aortic, and both common iliac areas (not shown), suggesting multiple lymph node and hepatic lymphoma involvement. After percutaneous ultrasound-guided needle biopsy, the mass was confirmed to be follicular lymphoma.

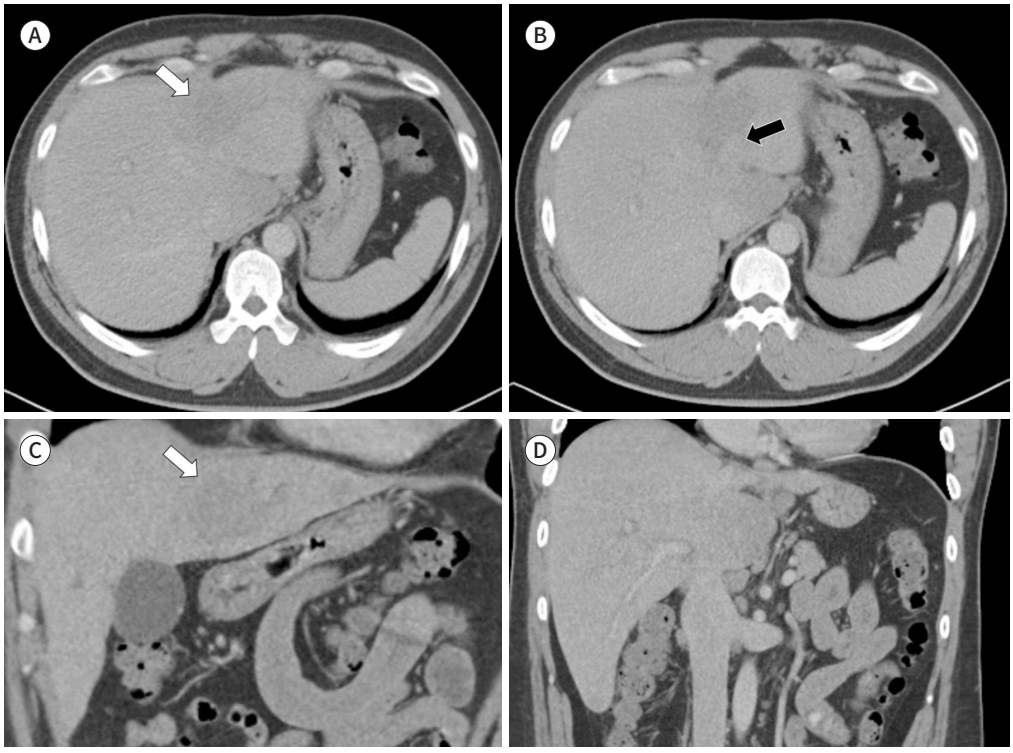

Fig. 15. Adrenal lymphoma in a 78-year-old female patient with anorexia.
A, B. On axial (A) and coronal (B) portal phase CT images, bilateral lobulated contour homogeneous masses are present in both the adrenal glands (11 cm and 8.5 cm in each), suggestive of adrenal lymphoma involvement. However, the mass was initially suggested as adrenal ganlioneuroma in the local clinic, and the patient was admitted to the endocrinology department in our hospital. Before formal radiologic report in our hospital, the patient underwent various screening tests for adrenal endocrine diseases, including serum and urine cortisol and serum adrenocorticotropic hormone, to assess adrenal insufficiency. After the report, the endocrinological test was discontinued, a percutaneous ultrasound-guided biopsy was performed, and the patient was diagnosed with high-grade B-cell lymphoma. Usually ganglioneuromas show well-circumscribed encapsulated margins and punctate or discrete calcifications, which is inconsistent with the findings in our case.

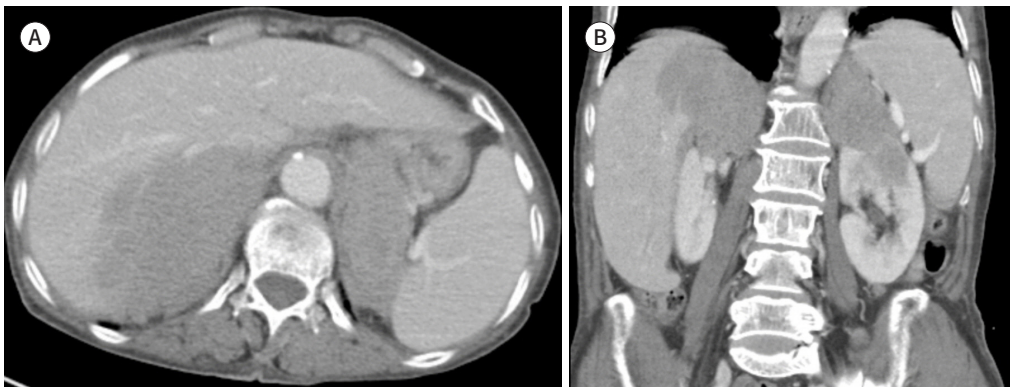

NHL cases (12, 30). Across all age groups, adrenal lymphoma is more common in patients with NHL than in those with HL. The main imaging feature is diffuse adrenal gland enlargement, which appears as a solid mass with a round, well-circumscribed homogeneous enhancement (12, 30). Approximately 50% of primary adrenal lymphomas occur bilaterally. Involvement of the adrenal gland in lymphoma can cause adrenal insufficiency. Therefore, the radiological interpretation of adrenal lymphomas is imperative for early treatment. If a radiologist interprets adrenal adenoma or other functional diseases from a lymphoma case, the patient may be admitted to the endocrinology department and undergo all endocrinology tests, and then finally get transferred to the hematology department (Fig. 15).

LYMPHOMA INVOLVING THE UTERUS

Uterine lymphomas are uncommon and account for approximately 2% of all extranodal and primary genital lymphomas in the female population (30, 34). The most frequent site of involvement is the uterine cervix. Imaging features of primary uterine lymphoma show diffuse uterine enlargement with homogeneous enhancement, despite the postmenopausal state (Fig. 16). Owing to its rarity, mimicking symptoms, and macroscopic findings similar to those of cervical carcinoma, only histopathological and immunohistochemical studies can

Fig. 16. Uterine lymphoma in a 78-year-old female patient with severe right leg edema.
A-C. Axial (A, B) and sagittal (C) CT images in the portal venous phase show mass-like lesions mainly in the anterior portion of the uterine cervix with lobulated contour and homogeneous enhancement. The lesion has also invaded the posterior wall and neck of the urinary bladder, urethra, bilateral distal ureter with bilateral hydronephrosis, and the anterior wall of the rectum.
D-G. Axial (D, E) and coronal (F, G) CT images in the portal venous phase show multiple homogeneously enlarged lymph nodes in the inguinal, iliac, aortocaval, and para-aortic areas. The right external iliac lymph node in the external iliac vein (white arrow) caused deep vein thrombosis of the right common femoral vein (black arrow). The patient was initially admitted to the department of vascular surgery for the management of right leg edema and transferred to the department of gynecology with suspected stage IV cervical cancer. The patient was menopausal and denied any gynecological symptoms, including vaginal discharge or abnormal uterine bleeding. The mass was confirmed to be high-grade B-cell lymphoma by performing punch biopsy of the uterus. Diagnosis before pathological confirmation is challenging because of the rarity of primary uterine lymphoma and the similarity in clinical symptoms of cervical carcinoma.

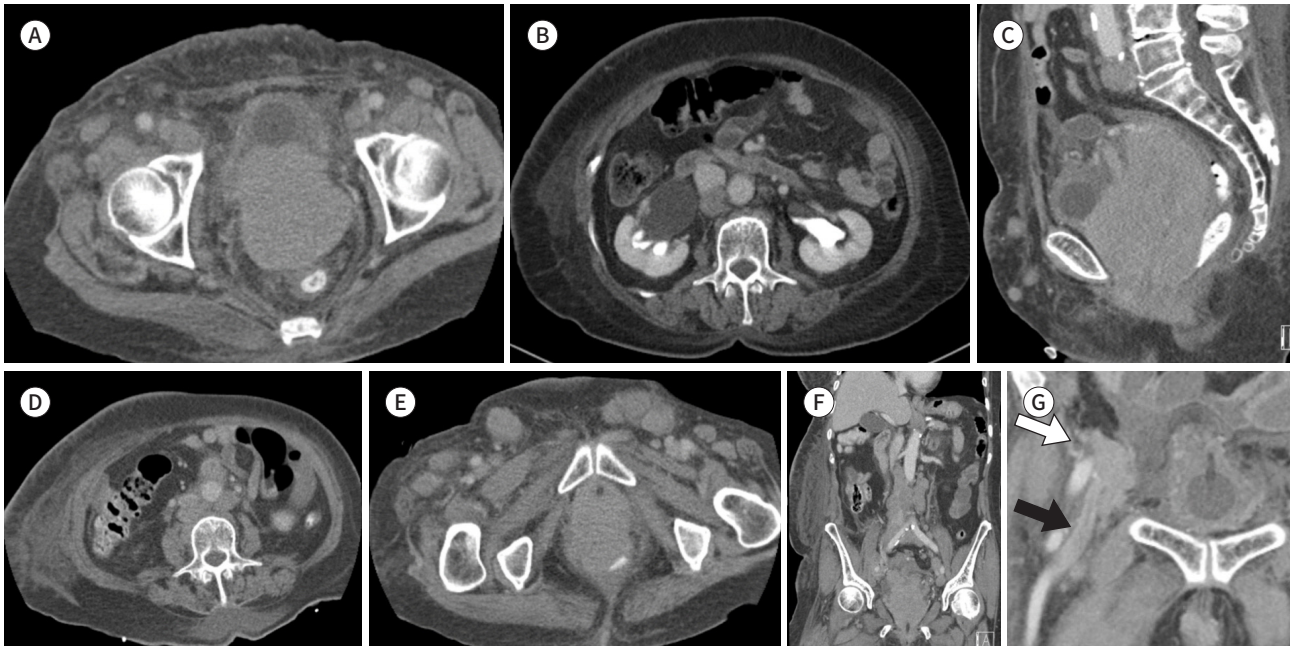

JOURNAL of
THE KOREAN SOCIETY of
RADIOLOGY

provide an accurate diagnosis (30, 34).

LYMPHOMA INVOLVING THE RETROPERITONEUM

Malignant lymphoma, a diffuse infiltrative form of the retroperitoneum, is a differential diagnosis of benign retroperitoneal fibrosis (3, 35). CT can provide a noninvasive routine evaluation of retroperitoneal lymphoma, although biopsy is considered the gold standard for accurate diagnosis (35). Malignant retroperitoneal lymphoma appears as a hypovascular infiltration or a bulky mass showing homogeneous attenuation surrounding the aorta and inferior vena cava (IVC) (Fig. 17). Lymphoma can involve the lymph nodes, which causes lymphadenopathy.

LYMPHOMA INVOLVING THE VESSEL

Intravascular large B-cell lymphoma (IVLBCL) is an uncommon type of extranodal diffuse

Fig. 17. A surgically proven retroperitoneal lymphoma in a 75-year-old male patient with acute abdominal pain.
A-D. Axial (A-C) and coronal (D) CT images in the portal venous phase show a large homogeneous retroperitoneal mass involving the pancreatic head and neck (white arrows), and the first and second portions of the duodenum (black arrows), encasing the portal vein without a malignant stricture and the gastroduodenal artery. Multiple variably sized round and oval enlarged lymph nodes without necrotic portions are also noted in the left gastric, peripancreatic, para-aortic, and aortocaval areas, suggestive of typical lymphoma involvement. Percutaneous ultrasound-guided biopsy of the abdominal mass confirmed diffuse large B-cell lymphoma.

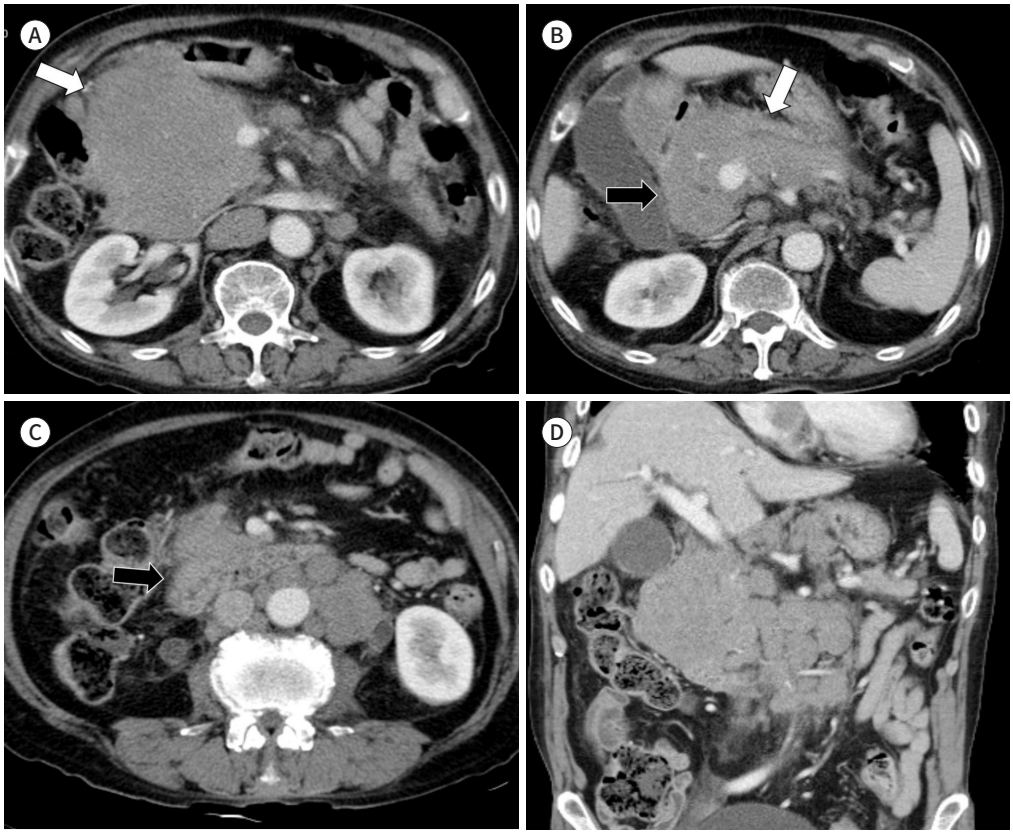

large B-cell lymphoma (36, 37). Three variants have been described based on clinical symptoms and outcomes (classical, cutaneous, and hemophagocytic syndrome-associated) (37, 38). In the classical variant, the symptoms are variable, including fever, pain, and specific symptoms depending on the organ involved. Intravascular lymphoma in the IVC appears as a homogeneous and minimally enhancing mass within the vessel (Fig. 18). In contrast, IVC leiomyosarcoma shows heterogeneous enhancement (39). Angiosarcomas also demonstrate heterogeneous enhancement and less commonly involve the retroperitoneum, particularly the IVC (39). In the cutaneous variant, the lesions are limited to the skin. The hemophagocytic syndrome-associated variant is the most aggressive form, involving hemophagocytosis in the bone marrow, liver, and spleen and has an unfavorable prognosis (38). However, the diagnosis of IVLBCL may be challenging, and several cases have been diagnosed on postmortem (36).

ENLARGED LYMPH NODES OR MASS MIMICKING LYMPHOMA

Various benign and malignant diseases can mimic lymphomas, including reactive lymphoid hyperplasia (Fig. 19), leukemia (Figs. 20, 21), HIV lymphadenitis (Fig. 22), desmoid tumors (Fig. 23), metastatic lymph nodes (Fig. 24), and other benign tumors (Fig. 25). Less ex-

Fig. 18. Intravascular lymphoma in a 73-year-old male patient with epigastric pain.
A-E. Axial (A, B), coronal (C), and sagittal (D) CT images in the portal venous phase present a 9.4 cm sized, homogeneously enhancing mass (white arrows) centered within the IVC. The tumor was initially suspected to be angiosarcoma with an extraluminal extension because of its location (around the IVC). However, the mass was diagnosed as high-grade B-cell lymphoma using fluoroscopy-guided transvenous biopsy. After review, another lesion is observed in the aortocaval area (E) with vessel infiltration without luminal narrowing (gray arrow), which is a typical feature of lymphoma.
IVC = inferior vena cava

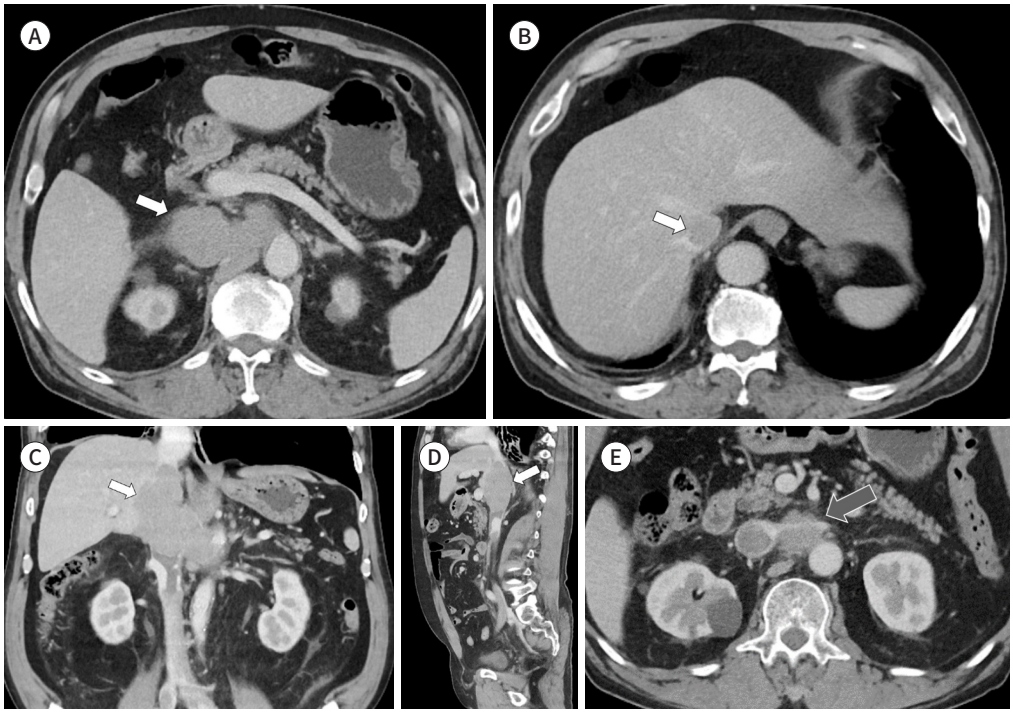

perienced physicians may misinterpret the collapsed small bowel as having enlarged lymph nodes and lymphoma involvement (Fig. 26). When radiologists become aware of various diseases that mimic lymphoma, they can easily differentiate lymphoma from other diseases. Understanding the imaging findings of lymphoma and mimicking diseases can help reduce unnecessary biopsies. Additionally, it enables quick and accurate treatment. Therefore, a

Fig. 19. Suggested benign lymphadenopathy in an 18-year-old male patient with acute abdominal pain.
A, B. On axial (A) and coronal (B) portal phase CT images, multiple prominent lymph nodes (arrows) measuring < 1 cm are observed in the ileocecal and mesenteric areas. Additionally, the patient had no previous medical history, and all laboratory results were within the normal range. These findings suggested benign lymphadenopathy and the patient was discharged after conservative treatment. No significant changes in lymphadenopathy were observed on serial 2 years follow-up CT scans.

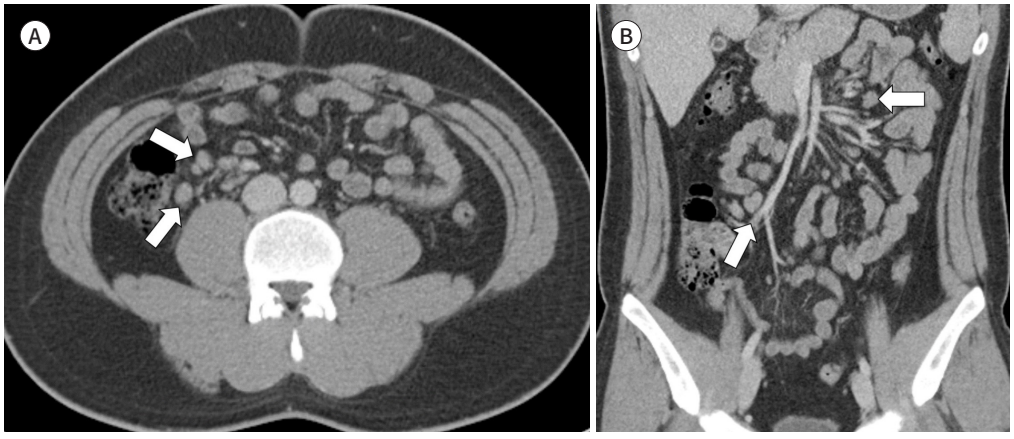

Fig. 20. Necrotic lymph nodes with acute myeloid leukemia in a 63-year-old female patient with a left palpable inguinal mass.
A, B. Axial (A) and coronal (B) portal phase CT images show enlarged lymph nodes with internal necrotic changes and perilymphatic infiltration in the left inguinal area. The findings were initially suggestive of lymphadenitis rather than pathological lymph nodes. However, 2%–3% of blasts with pancytopenia were detected on peripheral blood smear examination, suggestive of hematologic disorders. Bone marrow biopsy was performed, and the patient was diagnosed with acute myeloid leukemia. Lymphadenopathy associated with hematologic disorders can occur not only in lymphoma but also in leukemia.

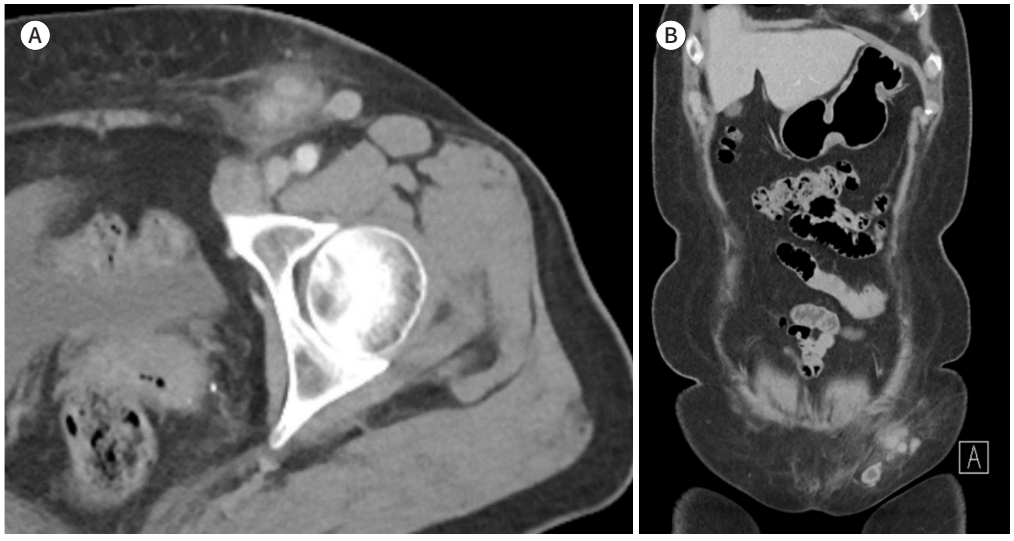

Fig. 21. Hepatic leukemia in a 49-year-old female patient with recent abdominal pain.
A, B. Axial (A) and coronal (B) CT images in the portal venous phase show several small, ill-defined, low-density lesions in the right hepatic dome. Several other small, ill-defined lesions were identified in both the hemilivers (data not shown).
C, D. Axial (C) and coronal (D) portal-phase CT images, multiple enlarged lymph nodes are present in the mesenteric, aortocaval, and para-aortic areas (arrows). Although the findings were initially suggestive of lymphoma with liver and lymph node involvement, acute myeloid leukemia was confirmed after bone marrow biopsy.

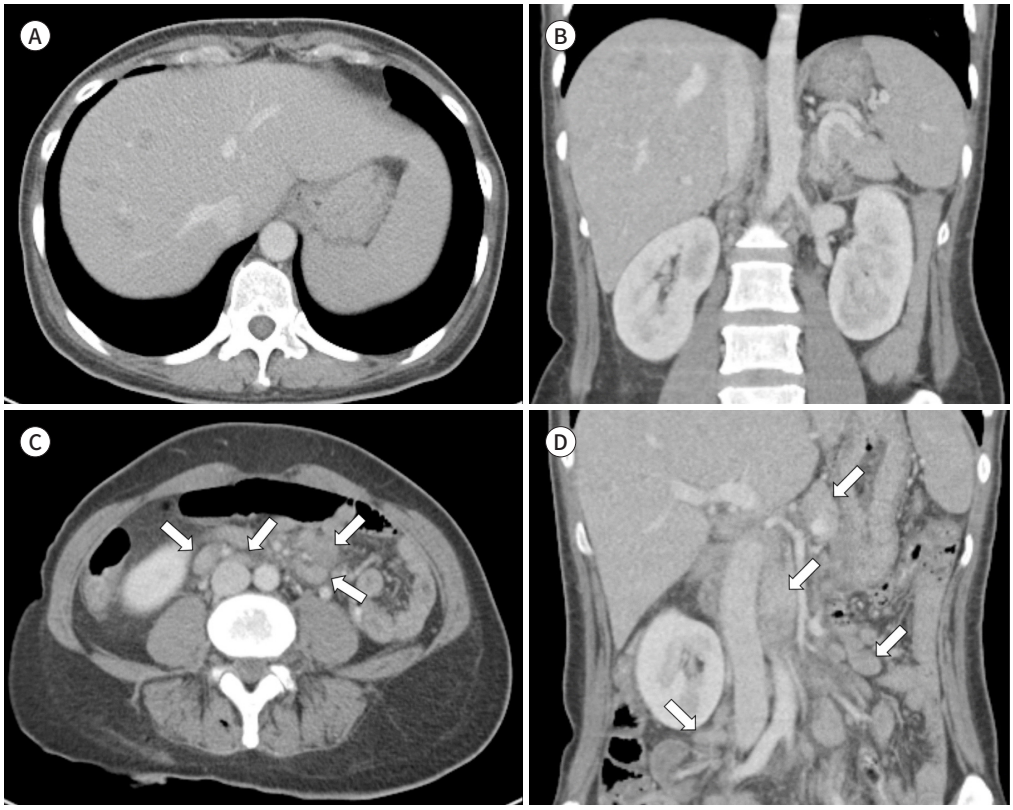

Fig. 22. HIV lymphadenopathy in a 33-year-old male patient with recent abdominal discomfort.
A-C. Axial (A, B) and coronal (C) CT images in the portal venous phase show multiple heterogeneously enhanced enlarged lymph nodes in the left gastric, common hepatic artery, retrocaval, paracaval, portocaval, para-aortic, and retropancreatic areas. Some lesions of the enlarged lymph nodes also contain an internal low-density (arrows). The patient also showed lymphadenopathy in both areas of the neck (not shown). As the patient did not have lung manifestations of tuberculosis, sarcoidosis or lymphoproliferative disease was initially suspected. The patient was diagnosed with HIV infection using polymerase chain reaction tests. In addition, an excisional biopsy confirmed lymphadenitis associated with HIV infection in the lymph nodes.
HIV = human immunodeficiency virus

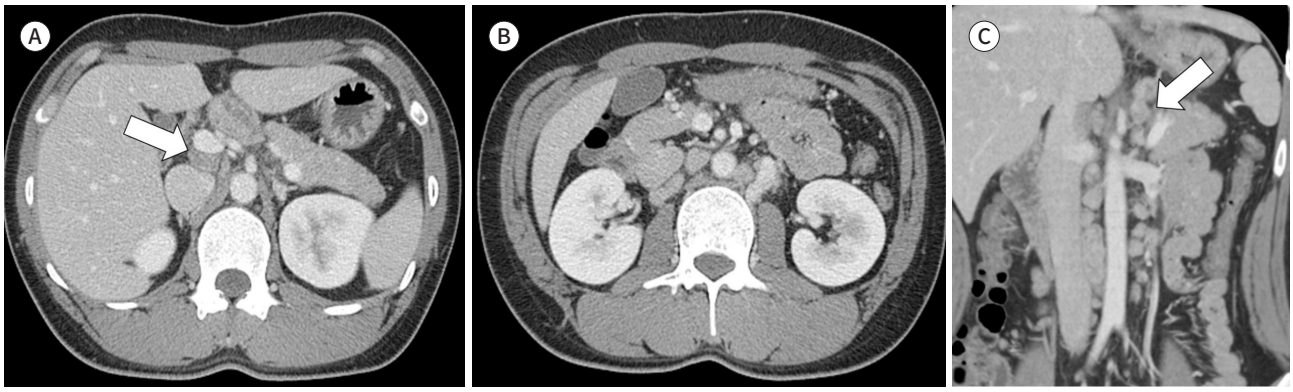

JOURNAL of
THE KOREAN SOCIETY of
RADIOLOGY

Fig. 23. Desmoid tumor in a 22-year-old male with recent periumbilical pain.
A-C. Axial (A, B) and coronal (C) CT images in the portal venous phase show a homogeneously enhancing mass with internal air bubbles and fluid collection in the right lower abdomen around the distal ileum. Additionally, multiple conglomerated, homogeneous, and enlarged lymph nodes were noted in the mesentery and para-aortic, aortocaval, portocaval, and paracaval areas. Differential diagnosis of the mass initially suggested desmoid tumor or lymphoproliferative disease involvement, including lymphoma. The patient underwent a percutaneous ultrasound-guided biopsy and was diagnosed with desmoid-type fibromatosis.

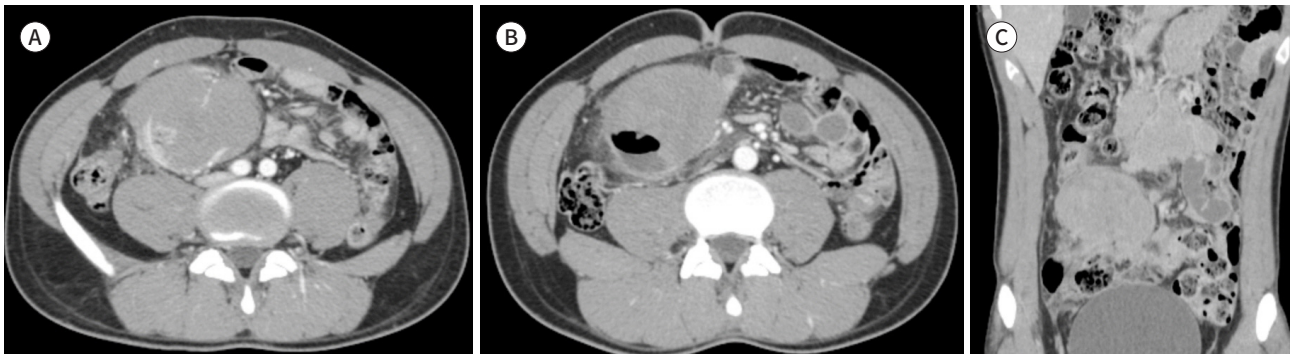

Fig. 24. Gallbladder cancer in a 55-year-old female with recent left abdominal pain.
A, B. Axial (A) portal venous phase and coronal (B) arterial phase CT images show multiple heterogeneously enhanced enlarged lymph nodes along the hepatoduodenal ligament, portocaval, aortocaval, and para-aortic areas. The lymph nodes in the hepatoduodenal ligament compress the inferior vena cava (arrow). Several enhancing nodular lesions are observed in the gallbladder body and neck. The findings were initially suggested retroperitoneal lymphoma involvement with compression of the common bile duct and cystic duct and combined gallbladder dilatation. However, the heterogeneity of lymph nodes with vascular compression and nodular lesions involving the gallbladder wall favored the diagnosis of gallbladder cancer. The patient underwent cholecystectomy and was diagnosed with mixed adenocarcinoma and neuroendocrine carcinoma of the gallbladder.

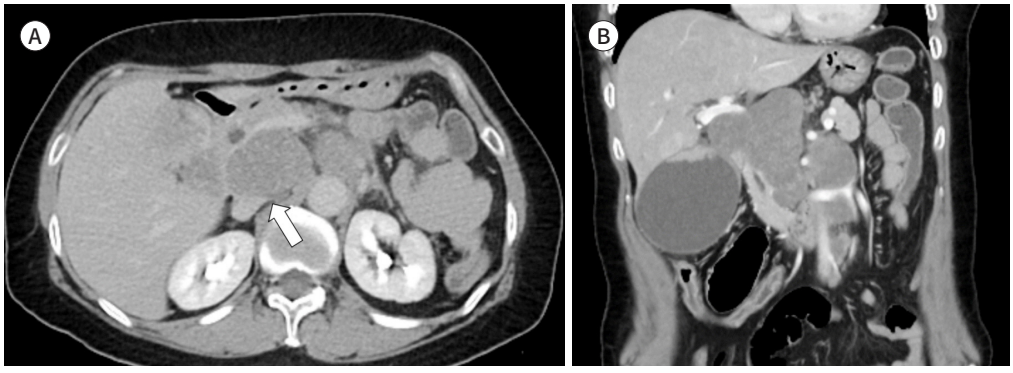

careful review of several imaging findings of these diseases can provide valuable insights for improving the diagnostic accuracy of lymphomas and other diseases that mimic them.

Enlargement of lymph nodes can occur because of infection, autoimmune diseases, and neoplasm. Careful history-taking, physical examination, and specific laboratory testing can help identify the possibility of infection or neoplasm. Specific B symptoms (fever, night sweating, and weight loss) without infection or a history of trauma are considered clues for lymphoma diagnosis. Generalized lymphadenopathy with firm and fixed lymph nodes > 2 cm in the short-axis diameter and homogeneous enhancement with splenomegaly generally suggests lymphoma involvement (10, 11).

Reactive lymphoid hyperplasia is a common etiology of lymphadenopathy and presents with

Fig. 25. Small bowel intussusception in a 78-year-old male with recent abdominal pain.
A-C. Axial (A, B) and coronal (C) CT images in the portal venous phase show soft tissue density in the proximal ileum (white arrows) associated with small bowel intussusception and mesenteric fat (black arrows). The radiologist initially interpreted small bowel intussusception caused by a small bowel mass, such as a lymphoma, as the leading point. However, after small bowel resection, the mass was diagnosed as an inflammatory fibroid polyp on surgical pathology. When reviewing the images again, the absence of lymph nodes around the intussusception was a key factor that helps to rule out the diagnosis of lymphoma.

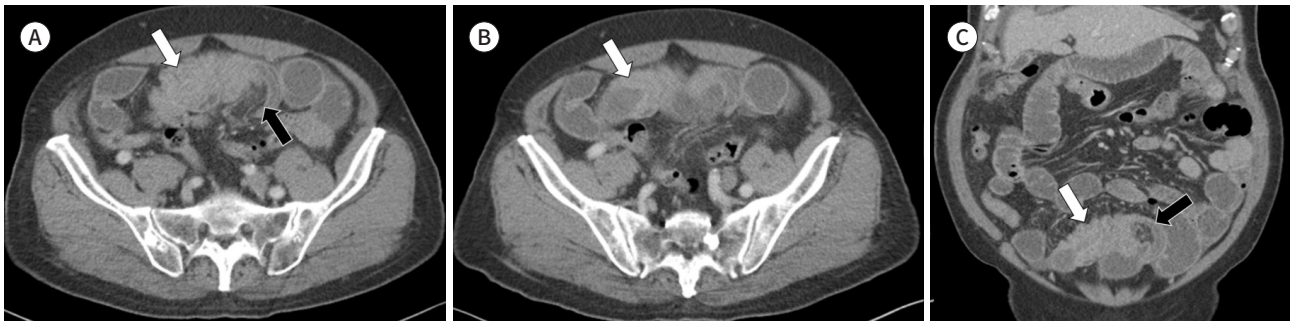

Fig. 26. Collapsed small bowel without enlarged lymph nodes in a 41-year-old female presenting with vomiting.
A, B. Less experienced physicians often misinterpret a collapsed small bowel as an enlarged lymph node. On the axial (A) and coronal (B) portal venous phase CT images, the collapsed jejunum (arrows) can bemisinterpreted as enlarged pathological lymph nodes by junior radiology residents.

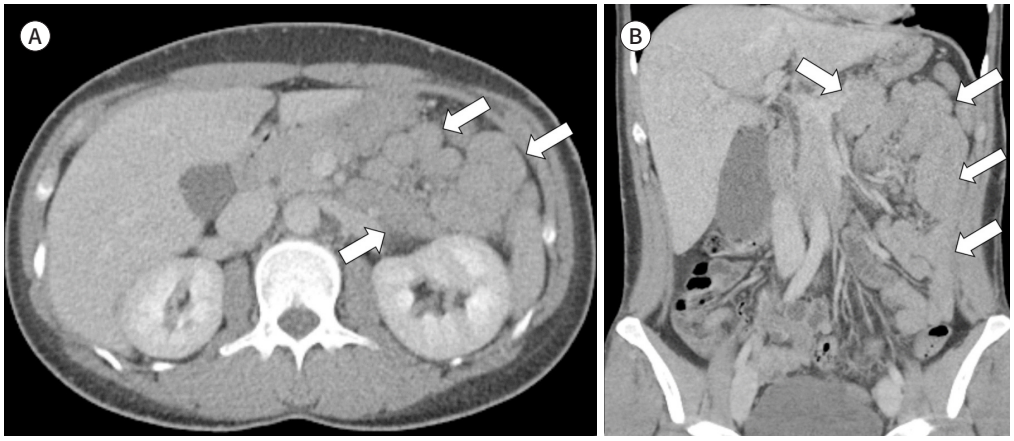

a short-axis diameter of < 1 cm (Fig. 19) (3, 40). If the findings are considered benign and self-limiting, conservative management and subsequent follow-up evaluations are offered (40).

Generalized lymphadenopathy involving two or more discrete anatomical regions can occur due to severe infections, autoimmune disorders, leukemia, lymphoma, or disseminated malignancy (3, 40, 41). The enhancement pattern of lymph nodes involved in leukemia and lymphoma is generally homogeneous (4, 41). However, lymph nodes associated with leukemia occasionally show peripheral enhancement with a thick rim or heterogeneous enhancement due to intranodal necrotic changes (Fig. 20) (41, 42). Leukemia mainly occurs in the bone marrow, whereas lymphoma affects the lymph nodes or extranodal organs (Fig. 21). Although some distinguishable characteristics exist between lymphoma and leukemia, an accurate diagnosis can only be made through histopathological examination (41).

Lymphadenopathy is a common manifestation of the acute stages of HIV infection. Tuberculosis is the most common cause of HIV-associated lymphadenopathy, followed by reactive

JOURNAL of THE KOREAN SOCIETY of RADIOLOGY

lymphadenitis. (Fig. 22) (43). Additionally, Kaposi's sarcoma and lymphoma are the most frequent malignant conditions in patients with HIV and can present with generalized lymphadenopathy (43, 44).

Intra-abdominal desmoid tumors are a subtype of desmoid tumors that account for approximately 8% of desmoid tumors. Although histologically benign, desmoid tumors can grow invasively and recur after excision. The common imaging features of desmoid tumors are well- or ill-defined masses with inhomogeneous enhancement within the mesentery and retroperitoneum on contrast-enhanced CT (Fig. 24); however, accurate diagnosis of the disease is challenging, as it can mimic lymphoma or malignant tumors with lymph node metastasis (45, 46).

Metastatic lymph nodes can be differentiated from lymphoma based on several factors, including a medical history of malignancy, specific enhancement pattern, and primary tumor adjacent to the lymphadenopathy. Metastatic tumors initially affect nearby lymph nodes, whereas hematopoietic cancers initially involve larger lymph nodes (41). Additionally, malignant lymphomas are aggressive and often involve extranodal sites at the time of initial diagnosis, but encase vessels without definite luminal narrowing (Fig. 24) (14, 41, 47).

An inflammatory myofibroblastic tumor (IMT) can also present similar to lymphoma and should be differentiated from lymphoma (48, 49). IMT is a rare mesenchymal spindle cell neoplasm that appears as a well-defined, homogeneous, or heterogeneously enhanced mass on CT. It commonly arises in the small intestine and is rarely associated with small bowel intussusception (Fig. 25) (48, 49). Similarly, lymphoma can be a leading cause of small bowel intussusception, making the differential diagnosis difficult (48, 50). However, the absence of enlarged perilesional lymph nodes is a key factor for differentiating lymphoma from other diseases.

CONCLUSION

The most common form of lymphoma is the lymph node form, which presents as homogeneously enhanced enlarged lymph nodes. However, various forms of nodal and extranodal lymphomas can occur in any part of the body. Therefore, it can be challenging to differentiate it from other diseases and accurately diagnose it. This study reviewed various features of lymphomas and several mimicking diseases, including benign lymphadenopathy, leukemia, HIV lymphadenitis, desmoid tumors, metastatic lymph nodes, and other primary malignancies. Because CT plays a major role in the accurate diagnosis of lymphoma, radiologists should be familiar with the typical and atypical features of lymphoma and other mimicking diseases to make a more precise diagnosis and provide early and accurate treatment interventions.

Author Contributions

Conceptualization, P.S.H.; data curation, P.S.H., Y.S.; formal analysis, K.J.E.; visualization, K.J.E.; writing—original draft, K.J.E.; and writing—review & editing, P.S.H., S.Y.S., Y.S.

Conflicts of Interest

The authors have no potential conflicts of interest to disclose.

Funding

None

REFERENCES

1. Jamil A, Mukkamalla SKR. Lymphoma. Available at. https://www.ncbi.nlm.nih.gov/books/NBK560826/?report=printable. Published 2021. Accessed January 15, 2023
2. Alaggio R, Amador C, Anagnostopoulos I, Attygalle AD, Araujo IBO, Berti E, et al. The 5th edition of the World Health Organization classification of haematolymphoid tumours: lymphoid neoplasms. *Leukemia* 2022;36:1720-1748
3. Frampas E. Lymphomas: basic points that radiologists should know. *Diagn Interv Imaging* 2013;94:131-144
4. Johnson SA, Kumar A, Matasar MJ, Schöder H, Rademaker J. Imaging for staging and response assessment in lymphoma. *Radiology* 2015;276:323-338
5. Krol AD, le Cessie S, Snijder S, Kluin-Nelemans JC, Kluin PM, Noordijk EM. Primary extranodal non-Hodgkin's lymphoma (NHL): the impact of alternative definitions tested in the Comprehensive Cancer Centre West population-based NHL registry. *Ann Oncol* 2003;14:131-139
6. Cheson BD, Fisher RI, Barrington SF, Cavalli F, Schwartz LH, Zucca E, et al. Recommendations for initial evaluation, staging, and response assessment of Hodgkin and non-Hodgkin lymphoma: the Lugano classification. *J Clin Oncol* 2014;32:3059-3068
7. Jiang H, Li A, Ji Z, Tian M, Zhang H. Role of radiomics-based baseline PET/CT imaging in lymphoma: diagnosis, prognosis, and response assessment. *Mol Imaging Biol* 2022;24:537-549
8. Li J, Wang J, Yang Z, Wang H, Che J, Xu W. Castleman disease versus lymphoma in neck lymph nodes: a comparative study using contrast-enhanced CT. *Cancer Imaging* 2018;18:28
9. Chae SY, Jung HN, Ryoo I, Suh S. Differentiating cervical metastatic lymphadenopathy and lymphoma by shear wave elastography. *Sci Rep* 2019;9:12396
10. Ferrer R. Lymphadenopathy: differential diagnosis and evaluation. *Am Fam Physician* 1998;58:1313-1320
11. Gaddey HL, Riegel AM. Unexplained lymphadenopathy: evaluation and differential diagnosis. *Am Fam Physician* 2016;94:896-903
12. Manzella A, Borba-Filho P, D'Ippolito G, Farias M. Abdominal manifestations of lymphoma: spectrum of imaging features. *ISRN Radiol* 2013;2013:483069
13. Hardy SM. The sandwich sign. *Radiology* 2003;226:651-652
14. Medappil N, Reghukumar R. Sandwich sign in mesenteric lymphoma. *J Cancer Res Ther* 2010;6:403-404
15. Wang HW, Balakrishna JP, Pittaluga S, Jaffe ES. Diagnosis of Hodgkin lymphoma in the modern era. *Br J Haematol* 2019;184:45-59
16. Adams HJA, de Klerk JMH, Fijnheer R, Dubois SV, Nievelstein RAJ, Kwee TC. Prognostic value of tumor necrosis at CT in diffuse large B-cell lymphoma. *Eur J Radiol* 2015;84:372-377
17. Hopper KD, Diehl LF, Cole BA, Lynch JC, Meilstrup JW, McCauslin MA. The significance of necrotic mediastinal lymph nodes on CT in patients with newly diagnosed Hodgkin disease. *AJR Am J Roentgenol* 1990;155:267-270
18. Saito A, Takashima S, Takayama F, Kawakami S, Momose M, Matsushita T. Spontaneous extensive necrosis in non-Hodgkin lymphoma: prevalence and clinical significance. *J Comput Assist Tomogr* 2001;25:482-486
19. Thomas AG, Vaidhyanath R, Kirke R, Rajesh A. Extranodal lymphoma from head to toe: part 2, the trunk and extremities. *AJR Am J Roentgenol* 2011;197:357-364
20. Olszewska-Szopa M, Wróbel T. Gastrointestinal non-Hodgkin lymphomas. *Adv Clin Exp Med* 2019;28:1119-1124
21. Lo Re G, Federica V, Midiri F, Picone D, La Tona G, Galia M, et al. Radiological features of gastrointestinal lymphoma. *Gastroenterol Res Pract* 2016;2016:2498143
22. Ghai S, Pattison J, Ghai S, O'Malley ME, Khalili K, Stephens M. Primary gastrointestinal lymphoma: spectrum of imaging findings with pathologic correlation. *Radiographics* 2007;27:1371-1388
23. Ciftci AO, Tanyel FC, Kotiloğlu E, Hiçsönmez A. Gastric lymphoma causing gastric outlet obstruction. *J Pediatr Surg* 1996;31:1424-1426
24. Levine MS, Rubesin SE, Pantongrag-Brown L, Buck JL, Herlinger H. Non-Hodgkin's lymphoma of the gastrointestinal tract: radiographic findings. *AJR Am J Roentgenol* 1997;168:165-172

25. Hashash JG, Habib-Bein N, Francis FF. MALT lymphoma causing gastric outlet obstruction. *ACG Case Rep J* 2015;2:70-71
26. Sandrasegaran K, Rajesh A, Rydberg J, Rushing DA, Akisik FM, Henley JD. Gastrointestinal stromal tumors: clinical, radiologic, and pathologic features. *AJR Am J Roentgenol* 2005;184:803-811
27. Lim CY, Ong KO. Imaging of musculoskeletal lymphoma. *Cancer Imaging* 2013;13:448-457
28. Scarisbrick JJ, Quaglino P, Prince HM, Papadavid E, Hodak E, Bagot M, et al. The PROCLIPI international registry of early-stage mycosis fungoides identifies substantial diagnostic delay in most patients. *Br J Dermatol* 2019;181:350-357
29. Sweet DE, Ward RD, Wang Y, Tanaka H, Campbell SC, Remer EM. Infiltrative renal malignancies: imaging features, prognostic implications, and mimics. *Radiographics* 2021;41:487-508
30. Anis M, Irshad A. Imaging of abdominal lymphoma. *Radiol Clin North Am* 2008;46:265-285, viii-ix
31. Nguyen T, Gupta A, Bhatt S. Multimodality imaging of renal lymphoma and its mimics. *Insights Imaging* 2022;13:131
32. Buyukpamukçu M, Varan A, Aydin B, Kale G, Akata D, Yalçin B, et al. Renal involvement of non-Hodgkin's lymphoma and its prognostic effect in childhood. *Nephron Clin Pract* 2005;100:c86-c91
33. Alves AMA, Torres US, Velloni FG, Ribeiro BJ, Tiferes DA, D'Ippolito G. The many faces of primary and secondary hepatic lymphoma: imaging manifestations and diagnostic approach. *Radiol Bras* 2019;52:325-330
34. Cubo AM, Soto ZM, Cruz MÁ, Doyague MJ, Sancho V, Fraino A, et al. Primary diffuse large B cell lymphoma of the uterine cervix successfully treated by combined chemotherapy alone: a case report. *Medicine (Baltimore)* 2017;96:e6846
35. Cronin CG, Lohan DG, Blake MA, Roche C, McCarthy P, Murphy JM. Retroperitoneal fibrosis: a review of clinical features and imaging findings. *AJR Am J Roentgenol* 2008;191:423-431
36. García-Muñoz R, Rubio-Mediavilla S, Robles-de-Castro D, Muñoz A, Herrera-Pérez P, Rabasa P. Intravascular large B cell lymphoma. *Leuk Res Rep* 2014;3:21-23
37. Ong YC, Kao HW, Chuang WY, Hung YS, Lin TL, Chang H, et al. Intravascular large B-cell lymphoma: a case series and review of literatures. *Biomed J* 2021;44:479-488
38. Ponzoni M, Campo E, Nakamura S. Intravascular large B-cell lymphoma: a chameleon with multiple faces and many masks. *Blood* 2018;132:1561-1567
39. Bednarova I, Frellesen C, Roman A, Vogl TJ. Case 257: leiomyosarcoma of the inferior vena cava. *Radiology* 2018;288:901-908
40. Bazemore AW, Smucker DR. Lymphadenopathy and malignancy. *Am Fam Physician* 2002;66:2103-2110
41. Zhang G, Yang ZG, Bai J, Li Y, Xu HY, Long QH. Leukemias involving abdominal and pelvic lymph nodes: evaluation with contrast-enhanced MDCT. *Abdom Imaging* 2014;39:1063-1069
42. Zhang G, Yang ZG, Yao J, Deng W, Zhang S, Xu HY, et al. Differentiation between tuberculosis and leukemia in abdominal and pelvic lymph nodes: evaluation with contrast-enhanced multidetector computed tomography. *Clinics (Sao Paulo)* 2015;70:162-168
43. Vanisri HR, Nandini NM, Sunila R. Fine-needle aspiration cytology findings in human immunodeficiency virus lymphadenopathy. *Indian J Pathol Microbiol* 2008;51:481-484
44. Riedel DJ, Rositch AF, Redfield RR, Blattner WA. HIV-associated lymphoma sub-type distribution, immunophenotypes and survival in an urban clinic population. *Leuk Lymphoma* 2016;57:306-312
45. Komatsu S, Ichikawa D, Kurioka H, Koide K, Ueshima Y, Shioaki Y, et al. Intra-abdominal desmoid tumor mimicking lymph node recurrence after gastrectomy for gastric cancer. *J Gastroenterol Hepatol* 2006;21:1224-1226
46. Sakorafas GH, Nissotakis C, Peros G. Abdominal desmoid tumors. *Surg Oncol* 2007;16:131-142
47. Hosoda K, Shimizu A, Kubota K, Notake T, Hayashi H, Yasukawa K, et al. Gallbladder Burkitt's lymphoma mimicking gallbladder cancer: a case report. *World J Gastroenterol* 2022;28:675-682
48. Cantera JE, Alfaro MP, Rafart DC, Zalazar R, Muruzabal MM, Barquín PG, et al. Inflammatory myofibroblastic tumours: a pictorial review. *Insights Imaging* 2015;6:85-96
49. Farhan M, Bibi A, Zulfiqar O, Imran M, Ali Z. Adult mid ileo-ileal intussusception secondary to inflammatory myofibroblastic tumor (IMT): a case report and literature review. *Cureus* 2020;12:e10902
50. Kim YH, Blake MA, Harisinghani MG, Archer-Arroyo K, Hahn PF, Pitman MB, et al. Adult intestinal intussusception: CT appearances and identification of a causative lead point. *Radiographics* 2006;26:733-744

J Korean Soc Radiol 2023;84(6):1266-1289

JOURNAL of THE KOREAN SOCIETY of RADIOLOGY

복부 악성 림프종의 영상 소견 및 비슷한 소견을 보일 수 있는 질병들

김종은 · 박소현* · 심영섭 · 윤성진

악성 림프종은 역동적 조영증강 컴퓨터단층촬영에서 전형적으로 커진 림프절 이 균일한 조영증강을 보이며 내부에 괴사 및 낭성 병변을 보이지 않는 영상 소견을 보이며, 이를 통해 침습적인 진단 검사 없이도 의심할 수 있다. 그러나 일부 림프종은 비전형적인 영상 소견을 보여 영상의학과 의사가 진단하는데 어려움을 겪는다. 더욱이, 실제 임상 현장에서는 백혈병, 면역저하자의 바이러스 감염, 원발암 및 전이암들이 림프종과 유사하게 보여 감별진단하는데 어려움이 있다. 초기에 영상검사로 악성 림프종과 이러한 유사질환을 구별하는것은 적절한 치료방침을 결정하는데 중요하다. 따라서, 본 임상 화보의 목표는 림프종의 전형적, 비전형적 영상 소견과 림프종을 모방하는 병변들의 영상 소견을 보여주며, 감별 진단을 좁히는데 도움이 되는 중요한 소견들을 논의하고자 한다.

가천대학교 의과대학 길병원 영상의학과

https://doi.org/10.3348/jksr.2023.0015